Hot Spots in Ag Core–Au Shell Nanoparticles Potent for Surface-Enhanced Raman Scattering Studies of Biomolecules

ARTICLE *in* THE JOURNAL OF PHYSICAL CHEMISTRY C · FEBRUARY 2007

Impact Factor: 4.77 · DOI: 10.1021/jp068253n

6 AUTHORS, INCLUDING:

Chandrabhas Narayana
Jawaharlal Nehru Centre for Advanced Scien…

155 PUBLICATIONS **1,714** CITATIONS

SEE PROFILE

Hot Spots in Ag Core−Au Shell Nanoparticles Potent for Surface-Enhanced Raman Scattering Studies of Biomolecules

G. V. Pavan Kumar,[†] S. Shruthi,[†] B. Vibha,[†] B. A. Ashok Reddy,[‡] Tapas K. Kundu,[‡] and Chandrabhas Narayana*[,†]

Light Scattering Laboratory, Chemistry and Physics of Materials Unit, Jawaharlal Nehru Centre For Advanced Scientific Research, Jakkur P. O. Bangalore-560064, India, and Transcription and Disease Laboratory, Molecular Biology and Genetics Unit, Jawaharlal Nehru Centre For Advanced Scientific Research, Jakkur P. O. Bangalore-560064, India

Received: December 1, 2006; In Final Form: January 25, 2007

The vicinity of metallic nanostructures that provides intense optical fields is termed as "hot spot". Any molecule in close proximity to these hot spots will give rise to an increased surface-enhanced Raman spectroscopic (SERS) signal. We have synthesized Ag core−Au shell (core−shell) nanoparticles (NP) with nanopores, which act as hot spots in the SERS measurements. We have demonstrated a large enhancement in SERS studies of various molecules using core−shell NP with hot spots, which is better than using silver nanoparticles. The core−shell NP with hot spots can be used for ultratrace analysis of important biomolecules such as histone acetyltranferase p300, a human transcriptional coactivator protein. The core−shell NP does not change the biomolecule's physical and chemical property upon adsorption, which makes it biocompatible. The core−shell NP carrying hot spots with high SERS enhancement would be ideally suited for in vivo studies of biological systems.

Introduction

Surface-enhanced Raman scattering (SERS) has emerged as one of the most potent analytical tools to probe different aspects of biology because of its high sensitivity and molecular detection capabilities.[1−10] In SERS, the Raman signal intensity of a molecule gets enhanced by many orders of magnitude when adsorbed to metallic nanostructures exhibiting atomic scale roughness.[11] The electromagnetic enhancement and the chemical enhancement are the two fundamental mechanisms for SERS. Most of the solution-phase experiments in SERS are performed using either Ag or Au nanoparticles. With Ag nanoparticles, one can obtain a very large enhancement in Raman intensities, but it is not preferred for in vivo studies in biological systems. In contrast, Au nanoparticles are used for in vivo studies of biological systems, but they provide moderate enhancement in SERS experiments. It is useful to think of a strategy to use the advantages of Ag and Au nanoparticles to benefit the studies of biomolecules.[12] Hence, we have carried out thorough investigations on the Ag core−Au shell (core−shell) nanoparticles (NP) as a possible SERS candidate for biological systems. Another important factor in core−shell NP is the possibility of a tunable surface plasmon resonance, which makes it an ideal candidate for wavelength-dependent studies.[13]

Recently, there has been a growing interest in understanding of the nature of SERS "hot spots" in various metallic nanostructures.[14−16] The hot spots facilitate enhanced optical fields, which in turn contribute to the electromagnetic enhancement when a molecule is in the vicinity of these spots. There have been various attempts to identify and design SERS hot spots. Some examples of these are (a) the Raman hot spots fabricated using on-wire lithography by Qin et al.,[15] (b) hot spots on Ag nanowire bundles by Lee et al.,[14] and (c) nanosphere arrays designed by Wang et al.[16] It is important to understand the basic methodology to produce these kinds of hot spots and tailor-make them for SERS applications. Core−shell nanoparticles could be one such candidate, where varying coverage of the shell could introduce hot spots by producing nanopinholes in the shell.[17]

In this report, we show that with proper manipulation of the Au shell in the core−shell NP we can produce the SERS hot spots. We also show the difference in SERS properties of core−shell NP with and without the hot spots and further demonstrate that one can use them to detect different kinds of biomolecules at nanomolar concentrations without the use of Raman markers as reported earlier.[12]

Experimental Details

Instrumentation. Transmission electron microscopy (TEM) experiments were performed using JEOL 3010 with an operating voltage of 300 keV. Field emission scanning electron microscopy (FE-SEM) was performed using Nova 600 NanoSEM (FEI, Germany). The ratios of Au to Ag were determined using energy dispersive X-ray analysis attached to the FE-SEM. UV−vis measurements were performed using Perkin-Elmer Lambda 900 UV/vis/NIR spectrometer. SERS measurements were performed using a custom-built Raman microscope whose details can be found elsewhere.[18] In the present experiment, the 632.8 nm wavelength of He−Ne laser was used as the excitation source. The laser power at the sample was ∼8 mW and the typical integration times were 10 s. All the SERS experiments were performed in aqueous conditions using a water immersion objective for focusing the laser and collecting the Raman signals.

* To whom correspondence should be addressed. E-mail: cbhas@jncasr.ac.in.
[†] Chemistry and Physics of Materials Unit.
[‡] Molecular Biology and Genetics Unit.

10.1021/jp068253n CCC: $37.00
Published on Web 03/01/2007

Chemicals. $AgNO_3$, trisodium citrate, $NH_2OH{\cdot}HCl$, and $HAuCl_4$ were bought from Merck, Germany. Rhodamine 6G (R6G), hemoglobin (Hb), myoglobin (Mb), and imidazole (Imd) were bought from Sigma Aldrich, United States.

Synthesis. The Ag colloids were prepared by the Lee and Meisel method.[19] Two hundred fifty milliliters of a 5.29×10^{-4} M $AgNO_3$ aqueous solution was brought to boiling with vigorous stirring, into which 5 mL of 1% trisodium citrate solution was added. The mixture was boiled for 1 h. The solution was allowed to cool to room temperature with continuous stirring. Core−shell NP was prepared by the seed growth method of Cui et al.[12] The core−shell NP with varying molar fractions of Au was prepared by the following method. A 12.5-mL Ag colloid solution was diluted with 10 mL of ultrapure water, and x mL of 6.25×10^{-3} M NH_2OH:HCl and x mL of 4.65×10^{-4} M $HAuCl_4$ were added dropwise (ca. 2 mL/min) by two separate pipets while vigorously stirring the mixture, where x is the concentration of Au desired in the final product. The stirring was continued for 45 min.

As a starting point of core−shell nanoparticle preparation, we have used a single batch of citrate-reduced Ag nanoparticles as the seed. The concentration of nanoparticles obtained by this method is around 10^{-4} M. Throughout the synthesis, to obtain different ratios of Au to Ag, the only parameter that was varied was the concentration of $HAuCl_4$, which would subsequently form the Au shell on Ag core. Apart from this, we also observed that the average particle density (500 ± 10 particles/μm^2) in the TEM image remained the same for all the samples.

Histone Acetyltransferase (HAT) Assay. The detailed procedure for extraction, purification, and activity testing of the human histone acetyltranferase p300 for SERS experiments can be found in earlier reports.[18,20] Briefly, 1.8 μg of highly purified HeLa core histones was incubated in HAT assay buffer containing 50 mM Tris-HCl, pH 8.0, 10% (v/v) glycerol, 1 mM dithiothreitol, 1 mM phenylmethylsulfonyl fluoride, 0.1 mM EDTA, pH 8.0, and 10 mM sodium butyrate at 30 °C for 10 min with or without baculovirus-expressed recombinant p300 in the presence and absence of nanoparticles followed by addition of 1 μL of 4.7 Ci/mmol [^{3}H] acetyl CoA (NEN-Perkin-Elmer) and was further incubated for another 10 min in a 30-μL reaction. The reaction mixture was then blotted onto P-81 (Whatman) filter paper, and radioactive counts were recorded on a Perkin-Elmer Wallac 1409 liquid scintillation counter. The typical concentration of p300 used for SERS was 40 ng/μL.

Results and Discussion

Figure 1 a−c shows the FE-SEM images of core−shell NP with Au to Ag ratio of 0.1, 0.4, and 0.8, respectively. There is a broad distribution in particle size (50 ± 20 nm), which is due to the size variation in Ag seeds prepared by the Lee and Meisel method. In the case of the core−shell NP, which has Au to Ag ratio of 0.4, we observe pinholes on the surface as shown by arrows in Figure 1b. These nanopinholes are formed because of the incomplete filling of Au shells over Ag nanoparticles. Hao et al.[17] and Alvarez-Puebla et al.[21] have earlier reported about pinholes in nanoshells prepared by different synthetic routes. These kinds of pinholes are usually formed in large numbers only for a particular ratio of Au to Ag (0.4, in our case), which is in agreement with the previous report by Cui et al.[12] Figure 1d shows the TEM image of the core−shell NP (Au to Ag ratio 0.4). The average sizes of these nanoparticles are ~50 nm for Au to Ag ratio equal to 0.4. The TEM image of Figure 1d shows a clear contrast between the core and the shell in the nanoparticles. The origin of the contrast in TEM

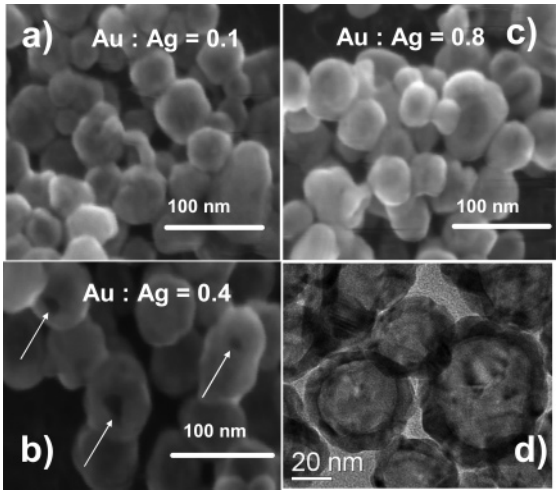

Figure 1. FE-SEM images of core−shell NP with Au to Ag ratio (a) 0.1, (b) 0.4, and (c) 0.8. (d) TEM image of core−shell NP shown in b. The arrows in b point to the nanopores on the surface of the gold shell which act as hot spots in the present experiments.

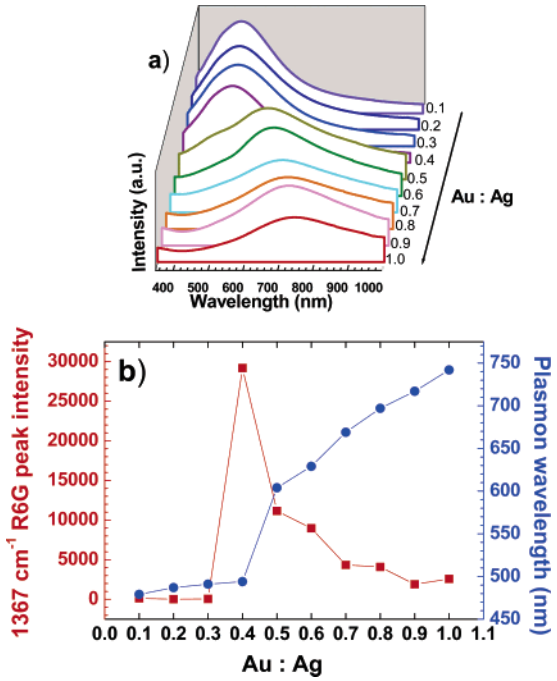

Figure 2. (a) UV−vis absorption spectra of core−shell NP as a function of Au concentration. (b) Double ordinate plot of intensity of the strongest Raman band (1367 cm^{-1}) of R6G (red) and the strongest plasmon absorption wavelength peak of a (blue) as a function of increasing Au concentration.

image has been previously studied in detail and is due to the presence of microtwining of the (111) plane of the gold over silver.[22] The present method used by us for the preparation of core−shell NP leads to a relatively uniform coating of the shell over the core (see Figure 1d) for Ag to Au ratios greater than 0.4, when compared to earlier methods.[17,21] This could have an added advantage of functionalizing the surface of the nanoparticles.

Figure 2a shows UV/vis absorption data for the core−shell NP with varying Au concentration. We observe a shift in the plasmon absorption of the core−shell NP as a function of the Au concentration, which shifts toward the red region of the electromagnetic spectrum. The UV/vis absorption spectra have a contribution from both Ag as well as Au plasmon absorptions, and the contribution shifts from Ag to Au as Au concentration

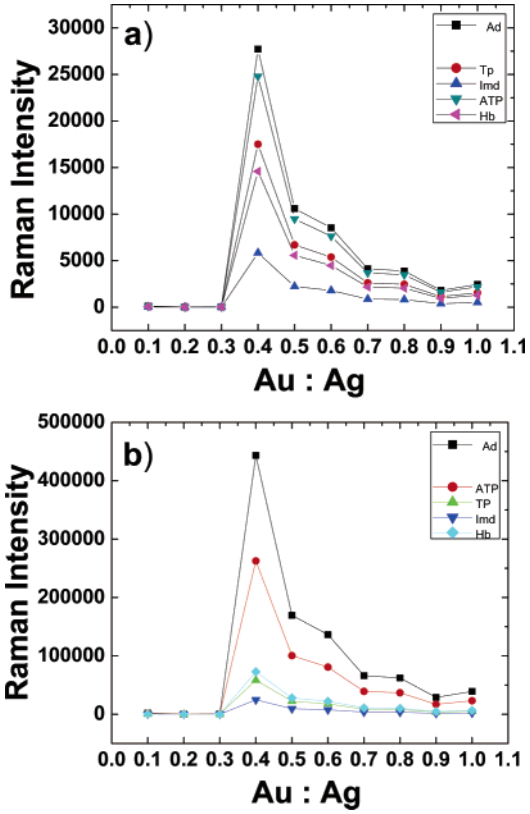

Figure 3. (a) SERS intensity as a function of Au to Ag ratio for adenine, Ad; thiophenol, TP; imidazole, Imd; adenosine triphosphate, ATP; and hemoglobin, Hb. Excitation wavelength used is 633 nm and accumulation time is 30 s. (b) SERS intensity as a function of Au to Ag ratio for the same molecules as mentioned above. Excitation wavelength used is 532 nm and the typical accumulation time is 10 s.

is increased. This behavior arises because of the increase in the thickness as well as the coverage of the Au shell around Ag nanoparticles as observed previously.[16,21,23] It was also observed that the particle size monotonically increased with increase in Au to Ag ratio. However, in some cases, for Au to Ag ratio greater than 0.7, it was observed that the particle size decreased (see Figure 1c). This might be because of the direct reduction of excess $HAuCl_4$ by $NH_2OH{\cdot}HCl$ to form pure Au nanoparticles along with the core−shell NP, which is the reason for the appearance of the small nanoparticles in the 0.8 case. We have performed SERS experiments on core−shell NP adsorbed with R6G for various ratios of Au to Ag. Figure 2b shows a double ordinate plot. Plasmon absorption wavelengths (blue) and the intensity of 1367 cm^{-1} band of R6G (red) are plotted as a function of increasing Au concentration. We observe that there exists a maximum in SERS intensity of the R6G Raman modes for the core−shell NP having a plasmon band peaking at ∼494 nm and Au to Ag ratio of 0.4. The absorbance values of the NP with pinholes at the laser (633 nm) and scattering wavelengths (which is at 683 nm for 1367 cm^{-1} band of R6G) were 0.62 and 0.46, respectively (see Supporting Information (SI) 1). For all the SERS experiments, the concentration of the nanoparticles were held constant (i.e., as synthesized without any further dilutions). We have not used any external aggregating agents like NaCl, KCl, and so forth. There was no appreciable difference in terms of aggregation after the R6G was adsorbed on different nanoparticles (see SI 2).

To provide stronger evidence to show that the above-mentioned SERS experiment does not depend on the molecule under supervision or on the Raman excitation frequency used, we have performed couple of experiments. At first, the

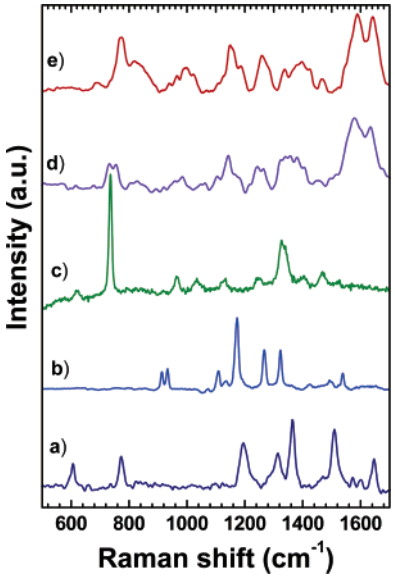

Figure 4. SERS spectra of (a) Rhodamine 6G, (b) imidazole, (c) adenosine triphosphate, (d) hemoglobin, and (e) myoglobin recorded with core−shell NP with hot spots (Figure 1b). The concentration of the biomolecules used for these experiments was 1 nM. Excitation wavelength of 632.81 nm and a power of ∼8 mW at the sample were used with a typical accumulation time of 10 s.

dependence of Raman signal intensity for different molecules (adenine, adenosine triphosphate, thiophenol, and hemoglobin) as a function of Au to Ag ratio was measured and plotted as shown in Figure 3a. It can be observed that the curve shows a maximum for Au to Ag ratio equal to 0.4 for a variety of molecules. This data indicates that the enhancement observed is not specific to a particular molecule and suggests that the pinholes in nanoparticles contribute to enhancement in Raman signal. Second, we performed the same experiment as mentioned above using a different excitation, namely, 532 nm. Figure 3b shows again a maximum for Au to Ag ratio equal to 0.4 for all the molecules. This data indicates that the enhancement observed is not wavelength specific and confirms that the contribution is mainly from the pinholes on nanoparticles. In the case of Au to Ag ratio of 0.4, we observe that almost all the nanoparticles appear with pinholes and that the Au shell coverage is nearly complete (see Figure 1b and d).

We can conclude that the pinholes are indeed acting as hot spots. The enhancement due to hot spots has been explained by Hao et al.,[17] who have shown by discrete dipole approximation (DDA) calculations that there would be a remarkable enhancement in the electric field at the vicinity of hot spots in Au nanoshells when compared to the seamless Au nanoshells. Discrete islands of Au shell on Ag core do not produce hot spots, as is the case of Au to Ag ratio below 0.4. It is known that the density of the hot spots plays an important role. If more than 10% of the surface area is covered with the hot spots, then the contribution of hot spots to SERS measurements could exceed that of the rest of the surface.[17] In our case, the formation of the nanopores on the surface for Au to Ag ratio of 0.4 leads to the hot spots and in turn results in enhanced Raman signal. The Raman enhancement factor for solution-phase experiments without any aggregating agent (like NaCl) was in the range of 10^8-10^9 (see SI 3).

Detection of Conventional Biomolecules in Nanomolar Concentrations Using Core−Shell NP with Hot Spots. Having identified the core−shell NP with hot spots, which lead to maximum enhancement in Raman signal intensity, we have used them to perform SERS on some of the conventional

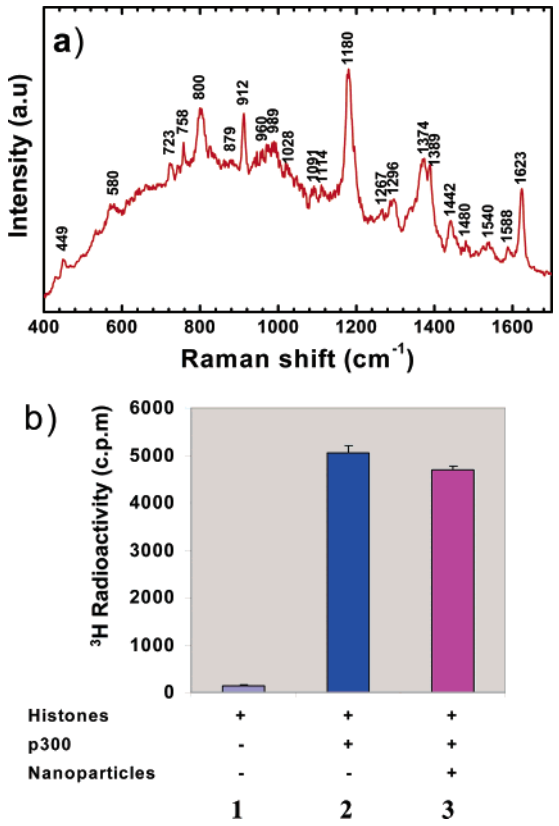

Figure 5. (a) SERS spectra of human transcriptional coactivator p300 using core−shell NP with hot spots (Figure 1b). The concentration of the protein used was 40 ng/μL and the typical accumulation time was 30 s. (b) Filter binding assay: HAT assay was performed by using highly purified HeLa core histones (800 ng) in the absence (lane 1) and presence (lane 2) of enzyme p300 (5 ng) and the enzyme (p300) incubated with core−shell NP with hot spots (lane 3). The results represent the average values with error bars from three independent experiments.

biomolecules like Mb, Hb (both are proteins), and adenosine triphosphate (ATP) along with R6G dye and Imd, which are extensively used in biology laboratories. Figure 4 shows the SERS spectra of all the above-mentioned molecules, which is in good agreement with the earlier reports.[24−28] We were able to perform these experiments at 1 nM concentration of the biomolecules without the use of external aggregating agent like NaCl or KCl. Normally, the aggregating agents are used to further enhance the Raman signals. In the SERS experiments with biomolecules, especially with the proteins in solution phase, the electromagnetic enhancement plays the major role in enhancing the Raman intensity.[29] SERS experiments on protein are rich in the information related to the ring-structured amino acids like phenylalanine, tyrosine, tryptophan, and so forth and the polypeptide backbone chains of the protein, since they interact strongly with metallic nanoparticles.[3,18,29] The presence of hot spots in core−shell NP would provide substantial enhancement to study the structure of the proteins in solution at low concentrations and in cases where the X-ray crystallographic data is absent. The structural information would be important in the protein−drug interaction studies too.

Detection of Nanomolar Concentration of Human Transcriptional Coactivator p300 Using Core−Shell NP with Hot Spots. Recently, we have performed a detailed SERS study[18] on human transcriptional coactivator p300 using Ag nanoparticles. p300 is a histone acetyl transferase (HAT) protein which regulates transcription mechanism in the human cell. The malfunctionality of this protein makes it an important target for therapeutics in several diseases. Therefore, it is important to understand the structure of the protein for applications in therapeutics. We have carried out the SERS experiments to determine the ability of core−shell NP with hot spots to detect and reveal the structural information of the p300 in solution phase at extremely low concentrations. Proteins such as p300 are very difficult to purify in large quantities, hence, this form of detection is very important to understand the structure−function relationship of the proteins. Figure 5a shows the SERS spectra of p300 at concentration 40 ng/μL performed using the core−shell NP. The Raman features are in agreement with the earlier reported work.[18] Since it was not possible to obtain the SERS using Au nanoparticles, we had performed the experiments using Ag nanoparticles.[18] The p300 spectra recorded in the present case have stronger intensities for the Raman modes in comparison to the ones using Ag nanoparticles. This clearly indicates that core−shell NP with hot spots could provide a technique to study ultratrace analysis and could be better than Ag nanoparticles for multiple reasons. It was important to verify that the histone acetyltranferase activity of p300 is unaffected by its adsorption to the nanoparticles, indicating that p300 structure is not modified by nanoparticles themselves while carrying out the SERS experiments. We have performed the filter-binding assay of the enzyme using highly purified human core histones.[18] Figure 5b shows that upon adsorption of p300 to core−shell NP with hot spots, the HAT activity of p300 is still intact. The data reveals that the enzyme in the solution as well as in the adsorbed state showed similar activity (Figure 5b, radioactive counts of lane 2 vs 3). Incubation of enzyme-adsorbed nanoparticles in the reaction system would have remote possibility to get detached from the nanoparticles in solution. Therefore, the activity observed from the nanoparticles containing the enzyme arises from the p300 molecules adsorbed onto the nanoparticles. Thus, all the above-mentioned experiments suggest that core−shell NPs with hot spots not only have the advantages of surface property of Au but also have enhancements larger than Ag nanoparticles, which could make them useful for in vivo biomolecular detection and analysis.

Conclusion

In summary, we have shown that core−shell NPs with pinholes act as hot spots that can greatly enhance Raman intensities of molecules (biological or otherwise) adsorbed onto it. The enhancement is mainly driven by the hot spot phenomenon described by Hao et al.[17] We have compared the core−shell NP with and without hot spots to suggest the importance of the hot spots in the enhancement of Raman signal. Core−shell NP with hot spots has been successfully used to detect different kinds of conventional biomolecules at nanomolar concentrations. We have also performed the SERS experiments using core−shell NP with hot spots on one of the therapeutically important human transcriptional coactivator p300 with a concentration of 40 ng/μL. It has been shown that the core−shell NP with hot spots does not affect the biological functionality of p300 by performing filter-binding assay. Thus, we conclude that core−shell NP with hot spots holds tremendous potential for determining the structure of biomolecules as well as applications in detection and therapeutics. Core−shell NPs with hot spots have advantage over Ag nanoparticles since they are better suited for in vivo experiments. By functionalizing the Au shells, one can use them in DNA discrimination and analysis. Work is under progress in this direction.

Acknowledgment. The authors thank Prof. G. U. Kulkarni and DST Unit for Nanoscience for helping us with providing

the FE-SEM facilities. S. S. and V. B. would like to thank the Project Oriented Chemical Education of JNCASR for providing the opportunity to undertake this project.

Supporting Information Available: Details of the absorbance values of the core−shell NP at the excitation and scattered wavelength, the figures showing the typical aggregation of the NP adsorbed with the probe molecule, and the details of the SERS enhancement calculations are provided. This material is available free of charge via the Internet at http://pubs.acs.org.

References and Notes

(1) Streltsov, S.; Oleinikov, V.; Ermishov, M.; Mochalov, K.; Sukhanova, A.; Nechipurenko, Y.; Grokhovsky, S.; Zhuze, A.; Pluot, M.; Nabiev, I. *Biopolymers* **2003**, *72*, 442−454.

(2) Stewart, S.; Fredericks, P. M. *Spectrochim. Acta, Part A* **1999**, *55*, 1641−1660.

(3) Podstawka, E.; Ozaki, Y.; Proniewicz, L. M. *Appl. Spectrosc.* **2004**, *58*, 1147−1156.

(4) Podstawka, E.; Ozaki, Y.; Proniewicz, L. M. *Appl. Spectrosc.* **2004**, *58*, 570−580.

(5) Ni, J.; Lipert, R. J.; Dawson, G. B.; Porter, M. D. *Anal. Chem.* **1999**, *71*, 4903−4908.

(6) Moore, B. D.; Stevenson, L.; Watt, A.; Flitsch, S.; Turner, N. J.; Cassidy, C.; Graham, D. *Nat. Biotechnol.* **2004**, *22*, 1133−1138.

(7) Kneipp, K.; Kneipp, H.; Itzkan, I.; Dasari, R. R.; Feld, M. S. *J. Phys.: Condens. Matter* **2002**, *14*.

(8) Graham, D.; Mallinder, B. J.; Smith, W. E. *Angew. Chem., Int. Ed.* **2000**, *39*, 1061−1063.

(9) Fabriciova, G.; Sanchez-Cortes, S.; Garcia-Ramos, J. V.; Miskovsky, P. *Biopolymers* **2004**, *74*, 125−130.

(10) Ermishov, M.; Sukhanova, A.; Kryukov, E.; Grokhovsky, S.; Zhuze, A.; Oleinikov, V.; Jardillier, J. C.; Nabiev, I. *Biopolymers* **2000**, *57*, 272−281.

(11) Moskovits, M. *Rev. Mod. Phys.* **1985**, *57*, 783−828.

(12) Cui, Y.; Ren, B.; Yao, J. L.; Gu, R. A.; Tian, Z. Q. *J. Phys. Chem. B* **2006**, *110*, 4002−4006.

(13) Prodan, E.; Nordlander, P. *Nano Lett.* **2003**, *3*, 543−547.

(14) Lee, S. J.; Morrill, A. R.; Moskovits, M. *J. Am. Chem. Soc.* **2006**, *128*, 2200−2201.

(15) Qin, L.; Zou, S.; Xue, C.; Atkinson, A.; Schatz, G. C.; Mirkin, C. A. *Proc. Natl. Acad. Sci. U.S.A.* **2006**, *103*, 13300−13303.

(16) Wang, H.; Levin, C. S.; Halas, N. J. *J. Am. Chem. Soc.* **2005**, *127*, 14992−14993.

(17) Hao, E.; Li, S.; Bailey, R. C.; Zou, S.; Schatz, G. C.; Hupp, J. T. *J. Phys. Chem. B* **2004**, *108*, 1224−1229.

(18) Kumar, G. V. P.; Reddy, B. A. A.; Arif, M.; Kundu, T. K.; Narayana, C. *J. Phys. Chem. B* **2006**, *110*, 16787−16792.

(19) Lee, P. C.; Meisel, D. *J. Phys. Chem.* **1982**, *86*, 3391−3395.

(20) Kundu, T. K.; Palhan, V. B.; Wang, Z.; An, W.; Cole, P. A.; Roeder, R. G. *Mol. Cell* **2000**, *6*, 551−561.

(21) Alvarez-Puebla, R. A.; Ross, D. J.; Nazri, G. A.; Aroca, R. F. *Langmuir* **2005**, *21*, 10504−10508.

(22) Srnova-Sloufova, I.; Lednicky, F.; Gemperle, A.; Gemperlova, J. *Langmuir* **2000**, *16*, 9928−9935.

(23) Bruzzone, S.; Malvaldi, M.; Arrighini, G. P.; Guidotti, C. *J. Phys. Chem. B* **2006**, *110*, 11050−11054.

(24) Bizzarri, A. R.; Cannistraro, S. *Appl. Spectrosc.* **2002**, *56*, 1531−1537.

(25) Chen, T. T.; Kuo, C. S.; Chou, Y. C.; Liang, N. T. *Langmuir* **1989**, *5*, 887−891.

(26) Etchegoin, P.; Liem, H.; Maher, R. C.; Cohen, L. F.; Brown, R. J. C.; Milton, M. J. T.; Gallop, J. C. *Chem. Phys. Lett.* **2003**, *367*, 223−229.

(27) Hildebrandt, P.; Stockburger, M. *J. Phys. Chem.* **1984**, *88*, 5935−5944.

(28) Muniz-Miranda, M.; Neto, N.; Sbrana, G. *J. Mol. Struct.* **1992**, *267*, 281−286.

(29) Chumanov, G. D.; Efremov, R. G.; Nabiev, I. R. *J. Raman Spectrosc.* **1990**, *21*, 43−48.